ADVANCED MATERIALS

Supporting Information

for *Adv. Mater.,* DOI: 10.1002/adma.202201042

Magnetic-Powered Janus Cell Robots Loaded with Oncolytic Adenovirus for Active and Targeted Virotherapy of Bladder Cancer

Zhaoqing Cong, Songsong Tang, Leiming Xie, Ming Yang, Yangyang Li, Dongdong Lu, Jiahong Li, Qingxin Yang, Qiwei Chen, Zhiqiang Zhang, Xueji Zhang, and Song Wu**

Supporting Information

Magnetic-Powered Janus Cell Robots Loaded with Oncolytic Adenovirus for Active and Targeted Virotherapy of Bladder Cancer

Zhaoqing Cong, Songsong Tang, Leiming Xie, Ming Yang, Yangyang Li, Dongdong Lu, Jiahong Li, Qingxin Yang, Qiwei Chen, Zhiqiang Zhang, Xueji Zhang, Song Wu**

*Corresponding Author. Email: tangsongsong@zxbiomed.org (S.T.); wusong@szu.edu.cn (S.W.)

Supporting videos:

Movie S1. Propulsion performance of 293T-R-Fe@OA cell robots under the RMF with different intensities

Movie S2. Propulsion performance of 293T-R-Fe@OA cell robots under the RMF with various frequencies

Movie S3. Propulsion performance of 293T-R-Fe@OA cell robots in various biological fluids

Movie S4. Propulsion performance of 293T-R-Fe@OA cell robots under a predefined square-like loop

Movie S5. Magnetic propulsion of 293T-R-Fe@OA cell robots against fluid flow

Movie S6. Controllable migration of 293T-R-Fe@OA cell robots in the microchannel

Experimental Section

Preparation of biotin-cRGD-FITC. 400 μM of FITC-labelled cRGD (cRGD-FITC; GL Biochem) was first dissolved in 1 mL of PBS. Then, Sulfo-NHS-biotin (0.5 mL, 200 μM, Macklin) was added to cRGD-FITC solution at the molar ratio of 1:2 and reacted for 1 hour. The resulting biotin-cRGD-FITC solution was stored at 4 °C until use.

Fabrication of 293T-R-Fe@OA cell robots. 293T cells (5×10^7 cells) were first cultured in a commercial 10-cm cell culture dish (Corning) for 6 hours and then infected with oncolytic adeno-D55-CMV virus (OA, Fubio, OVAD-0145) at the MOI of 64 for another 12-hour incubation. Afterward, the suspension was removed and 293T cells infected with OA (293T@OA) were washed with PBS (pH 7.4) three times to remove free virus. The resulting 293T@OA were harvested in PBS and stored at 4 °C for subsequent modifications.

The collected 293T@OA (5×10^7 cells) were sequentially reacted with Sulfo-NHS-biotin (200 μM, Macklin), Cy3-labelled streptavidin (200 μM, Sigma-Aldrich), and biotin-cRGD-FITC (described above) for 1 hour. Three-time washes were required to remove free agents for each step. The synthesized 293T-R@OA were dispersed in PBS and stored in 4 °C until use.

Before the Janus modification, Fe_3O_4 NPs (Macklin) were mixed with TA solution (0.4 mg/mL in 0.5 × PBS, Sigma-Aldrich) for 4 hours and then washed with PBS twice. The prepared 293T-R@OA were incubated in a commercial 6-well plate coated with PLL (Corning) for 6 hours to attach with the plate bottom and partially block the cell membrane. The suspension was then removed, and the plate was rinsed three times with PBS to eliminate unattached cells. Subsequently, TA-treated Fe_3O_4 NPs solution (3 mL, 100 μg/mL) was added to the plate. After 5-min incubation, the solution of PDBA (500 μL, 42 μM, Sigma-Aldrich) was added and incubated with gentle shaking for 10 s. Last, the resulting 293T-R-Fe@OA cell robots were washed with PBS three times and detached from the PLL-modified bottom through repeatedly and mildly pipetting. The released cell robots were rinsed with PBS twice and stored in 4 °C until use.

Characterization of cell robots. The surface charge of all steps was measured by Malvern Panalytical Zetasizer Nano ZS90. The average size was calculated by measuring 50 cells under optical microscope (ECLIPSE Ti2-U, Nikon, Japan). The cRGD modification was characterized by optical and fluorescent images of cell robots with Cy3-labeled streptavidin and cRGD-FITC, captured using a confocal laser scanning microscopy (Zeiss Axio Observer, Carl Zeiss, Oberkochen, Germany). Flow cytometry analysis was performed to explore the feasibility and efficiency of such modification using Becton Dickinson FACSAria II flow cytometer. SEM and EDX images were conducted on a Thermo APREO S SEM with an accelerating voltage of 5.0 and 15.0 kV, respectively. X-ray Photoelectron Spectrometer (XPS) images were conducted on a Thermo Scientific ESCALAB 250Xi Microprobe.

Regarding the viability of cell robots after cell surface modification, cell robots and 293T@OA at the same cell concentration of 5×10^4 cells/mL were sequentially stained with PI (3 μM) and Hoechst 33324 (1 μM) for 30 min at 37 °C. After three times wash with PBS, fluorescent images of cells were captured using a confocal laser scanning microscopy (Zeiss Axio Observer), where dead or live cells represent red color from PI or blue color from Hoechst 33324, respectively.

Oncolytic effect of OA to various cancer cell lines. Various cancer cells, including T24, 5637 bladder cancer cells, HeLa cervical cancer cells and T47D breast cancer cells, were seeded in 96-well plate at the density of 3×10^3 cells per well and incubated overnight. Then, cancer cells were infected with OA upon various MOIs (0.1, 2, 10, 50, 100 and 500). The cell viability was measured after different postinfection periods (24, 48 and 72 hours) using Cell-Counting Kit-8 (CCK8) assay (Yeasen Biotech). Spark Multimode Microplate Reader (TECAN) was used to measure the absorbance at 450 nm.

Viral replication and cytolytic effect of OA loaded in 293T cells. To explore the cytolytic and replicative capability of OA in 293T cells, 293T cells were seeded in 96-well plate at the density of 3×10^3 cells per well and incubated overnight. Then, 293T cells were infected with GFP reporter gene-engineered OA, adeno-D55-CMV-EGFP (GFP-OA, Fubio, FV145) upon various MOIs (2, 4, 8, 16, 32, 64, 128, 256, 512 and 1024). The viability of 293T cells was measured after different postinfection periods (24 and 48 hours) using CCK8 assay. The OA-infected 293T cells can express GFP due to the inserted GFP reporter gene in OA, where the GFP fluorescence

intensity can be quantified to represent the replication level of OA. The fluorescent images of 293T cells were captured using a confocal laser scanning microscopy (Zeiss Axio Observer).

To evaluate the effect of cell surface engineering on the replicative level of OA in 293T cells, the fabricated 293T@OA and 293T-R-Fe@OA cell robots were cultured in a 12-well plate at the same density of 5×10^4 cells/well. After incubated for 48 hours, total RNA inside cells and culture medium were extracted using TRIzol (258311, Ambion). In each instance, 2 μg of purified mRNA was reversely transcribed to DNA using the Discover-sc WTA Kit V2 kit (Vazyme) and amplified using the SYBR Green quantitative PCR kit (Invitrogen, Carlsbad, CA). Such process was performed in triplicate. The calculation method of $2^{-\Delta\Delta CT}$ described in the following equations (Eq. 1-Eq. 3) was used to determine the relative gene expression level of different samples using the threshold cycles (CTs) generated by the qPCR system. The housekeeping gene, glyceraldehyde 3-phosphate dehydrogenase (GAPDH), was used as reference gene and the expression level inside cells of the 293T@OA group was normalized to 1.0.

$$\Delta C_T = C_{T\ E1A} - C_{T\ GAPDH} \quad (1)$$

$$\Delta\Delta C_T = \Delta C_T - \Delta C_T\,(293T@OA\text{-}Cell) \quad (2)$$

$$\text{Relative Quantification (RQ)} = 2^{-\ \Delta\Delta CT} \quad (3)$$

To assess the impact of cell surface engineering on the oncolytic effect of OA in 293T cells, T24 cancer cells (3×10^3 cells) were seeded in a 96-well plate and incubated overnight. 10 μL of PBS, free OA, 293T@OA and 293T-R-Fe@OA cell robots were added to the plate at a cell density of 3×10^3 cells/mL. The dosage of free OA was 64 MOI, equal to the OA amount in infecting 293T cells to build 293T@OA and cell robots. The viability of T24 cells were measured using CCK8 assay after various incubation durations (24, 48, 72 and 96 hours).

To examine the viability of 293T@OA and 293T-R-Fe@OA cell robots upon elongated incubation, 293T@OA and cell robots were fabricated using two MOIs of OA (64 and 128) and cultured in a 96-well plate at a cell density of 3×10^3 per well. The cell viability was measured after 3, 4, 5 and 6 days postinfection using CCK8 assay.

Specific binding between cell robots and bladder cancer cells. 293T@OA, 293T-R@OA and 293T-R-Fe@OA cell robots (6×10^5 cells/mL) were first labelled with DiD (1 μg/mL) for 45 min at room temperature, then washed with PBS three times to remove free dyes. DiD-labelled 293T@OA, 293T-R@OA and cell robots were incubated with GFP-expressing T24 cancer cells for 1 hour, followed with PBS wash for two times to remove unattached cells. The binding between T24 cells with 293T@OA, 293T-R@OA or cell robots were characterized by fluorescent images captured using a confocal laser scanning microscopy (Zeiss Axio Observer).

Propulsion investigation of magnetic-powered cell robots. The cell robots were propelled and navigated using a home-made magnetic actuation system consisting of control and power units. The LabVIEW software (version 18.0, National Instruments) in a host computer works as the control unit and generate the digital signal. Such signal is translated to the analog signal by a data collection card (USB DAQ V1.2, Hengkai Electronic Technology) and sent to the power amplifier (TDA8954, NXP Semiconductors) for signal amplification. Then, 5 electromagnetic coils (a pair of coils in X and Y axis and one coil in Z axis) placed under an optical microscopy receive the amplified analog inputs and generate desired rotating magnetic field.

The propulsion study of cell robots was performed in PBS solution. An optical microscope linked with a charge-coupled device (CCD) camera (MS23-2, Guangzhou Mshot photoelectric technology) was connected to the computer to capture motion videos, which were further analyzed with NIS-Elements AR 5.21.02 software.

Simulation method of magnetic propulsion. Simulation of the fluid flow induced by the rolling of Janus cell robot was conducted using finite element analysis (FEA) on the COMSOL Multiphysics 5.6 software. Tetrahedral elements with refined meshes allowed modeling of the fluid flow field in 3D space with testified accuracy. The fluid flow is described by Navier-Stoke equation for incompressible flow:

$$\rho\left(\frac{\partial v}{\partial t} + (v \cdot \nabla)v\right) = -\nabla p + \mu\nabla^2 v$$

$$\nabla \cdot v = 0$$

Where ρ, v, p and μ denote liquid density, flow velocity, pressure and viscosity, respectively.

In the model, the cell robot with radius of $a = 7.5$ μm is set at $\delta = 1$ μm from the substrate. The rotating magnetic frequency was set as 5 Hz. A no-slip boundary condition was applied to the surface of cell robot and substrate.

Magnetic movement of cell robots against fluid flow. The motion study against fluid flow was conducted using a microfluidic chip with microchannels at the diameter of 500 μm. The PBS solution containing Janus cell robots and free 293T cells were injected to the microfluidic device using the syringe pump to mimic blood flow. The flow rate was controlled at 400 μm/s. The magnetic motion of cell robots inside the microchannel was observed and recorded using an optical microscope linked with CCD camera.

***In vitro* migration of magnetic-propelled cell robots in a microfluidic device.** The microfluidic device is composed of two 10 × 10 mm square reservoirs connected by four microchannels with the axial length of 10 mm, where the diameter of two microchannels are 0.5 mm and another two are 1 mm. T24 cancer cells (1×10^4 cells) were first seeded on the right reservoir for 6-hour incubation. Then, Cy3-labelled 293T-R-Fe@OA cell robots were added to the left chamber and treated without or with RMF control for 5 min. The fluorescent images of Cy3-labelled cell robots in the microfluidic chip were captured using Near-Infrared Fluorescence Imaging System (LI-COR, Odyssey CLx). The viability of T24 cells was measured by CCK8 assay after incubated with the migrated cell robots for various durations (24, 48 and 72 hours).

Controllable locomotion of cell robots in the bladder mold. A urinary system mold containing bladder chamber with a lateral and longitudinal diameter of 50 mm and 40 mm, respectively, was used in this experiment. Cy3-labeled 293T-R-Fe@OA cell robots (5×10^7 cells) were added to the bladder chamber and treated without or with RMF control for different durations (0, 2, 5 and 10 min). The optical and fluorescent images presenting the distribution of cell robots inside bladder mold were captured using Near-Infrared Fluorescence Imaging System (LI-COR, Odyssey CLx).

Animals. BALB/c nude mice (female, six-weeks old) were purchased from GemPharmatech Co., Ltd. All animal experiments were strictly conducted in compliance with the guidelines of Animal Use and Care Administrative Advisory Committee of Shenzhen Luohu Hospital Group.

Magnetic steering of cell robots in mice bladder. Upon the *in vivo* manipulation of cell robots in mouse bladder, the PBS solution containing 293T-R-Fe@OA cell robots (5×10^7 cells) were intravesically injected to the BALB/c nude mice bladder from urethra via a closed IV catheter system (0.7 mm × 19 mm, BD Intima II). For both *ex vivo* and *in vivo* imaging, the mice were processed without or with RMF control (10.3 mT, 17 Hz) for 1 hour. For the *ex vivo* imaging, the mice were sacrificed after intravesical administration for 5 min and 60 min. The urinary system was dissected to capture fluorescent images using Near-Infrared Fluorescence Imaging System (LI-COR, Odyssey CLx). Regarding the *in vivo* imaging, the mice was further free incubated for another 5 hours after the 1-hour intravesical administration. The image was captured at the timepoint of 0.1 hour and 6 hours using Near-Infrared Fluorescence Imaging System (LI-COR, Odyssey CLx).

***In vitro* tissue penetration and anticancer efficacy of cell robots to 3D cell spheroid.** T24 cells were seeded in a 96-well plate with the ultra-low attachment surface at a density of 1.2×10^3 cells per well. After incubated for 5 days, the cell spheroid formed in the bottom of each well and was then incubated with GFP-OA, 293T@OA, 293T-R@OA, 293T-R-Fe@OA, F-293T, 293T-R-Fe@OA with RMF control and 293T-R-Fe@OA under magnetic shaking at the same cell density of 1×10^4 cells/mL for 1 hour. The dosage of free GFP-OA was 64 MOI, the same as the GFP-OA dose to infect 293T cells for subsequent modification. Afterward, the plate was washed with PBS and added fresh DMEM for another 48-hour incubation. Last, T24 cell spheroids were stained with PI (3 μM) for 30 min and washed with PBS three times. The fluorescent images of transverse sections of T24 cell spheroids at different depths were captured using a confocal laser scanning microscopy (Zeiss Axio Observer).

***In vivo* antitumor study of cell robots.** The orthotopic bladder tumor model was established by surgically injecting 20 μL of PBS containing luciferase-expressing T24 bladder cancer cells (1×10^6 cells) into the bladder wall of each mouse under anesthetization via a 0.33 mm × 12.7 mm insulin syringe (Becton, Dickinson, and Company). Seven days after the cell inoculation (day 0), mice bearing T24 bladder tumor were randomly divided to 6 groups (n = 5) and intravesically injected with PBS (negative control), PBS solution containing OA, 293T@OA, 293T-R@OA, 293T-R-Fe@OA cell robots, and 293T-R-Fe@OA cell robots upon RMF control at the same volume of 200 μL through a closed IV catheter system (0.7 mm × 19 mm, BD Intima II). The

cell concentration of each group was 5×10^7 cells. The virus dosage was 64 MOI for free OA group and infecting 293T cells toward sequential cell surface modification. The duration of such intravesical administration was 1 hour, where the mice were anesthetized in this process. For group of "293T-R-Fe@OA + RMF", the mice after intravesical instillation of cell robots were placed under the magnetic field (10.3 mT, 17 Hz) for 1 hour. Such intravesical administration were performed every two days for three times (day 0, 2 and 4). The period of such treatment was 14 days (day 13). The orthotopic tumor growth was monitored by the bioluminescence on mice every two days imaged using an IVIS Lumina system (Caliper Life Sciences) and the body weight of mice were recorded every two days during the treatment course. The intensity and area of detected bioluminescence on mice were quantified by Living Image (PerkinElmer, version 4.5). After finishing the treatment, mice were sacrificed and bladders were excised and processed with H&E staining for histological characterization of tumor growth. The stained bladder sections were visualized using digital pathology slide scanner (KF-PRO-005 EX, KFBio). Major organs of mice, including kidney, spleen, lung, heart and liver, were also dissected and imaged using an IVIS Lumina system (Caliper Life Sciences) to detect the bioluminescence for the examination of cancer metastasis.

Statistical Analysis

All data are presented as mean ± standard deviation (SD). Statistical analysis was performed with a minimum sample size of 3. Statistical comparisons of two groups were conducted using Student's t-test. One-way analysis of variance (ANOVA) with Turkey's posthoc analysis was used to determine the significance between three or more groups. All statistical analysis was evaluated using GraphPad Prism 8. *$p < 0.05$ stands for significant and **$p < 0.01$ represents very significant.

Supporting Figures:

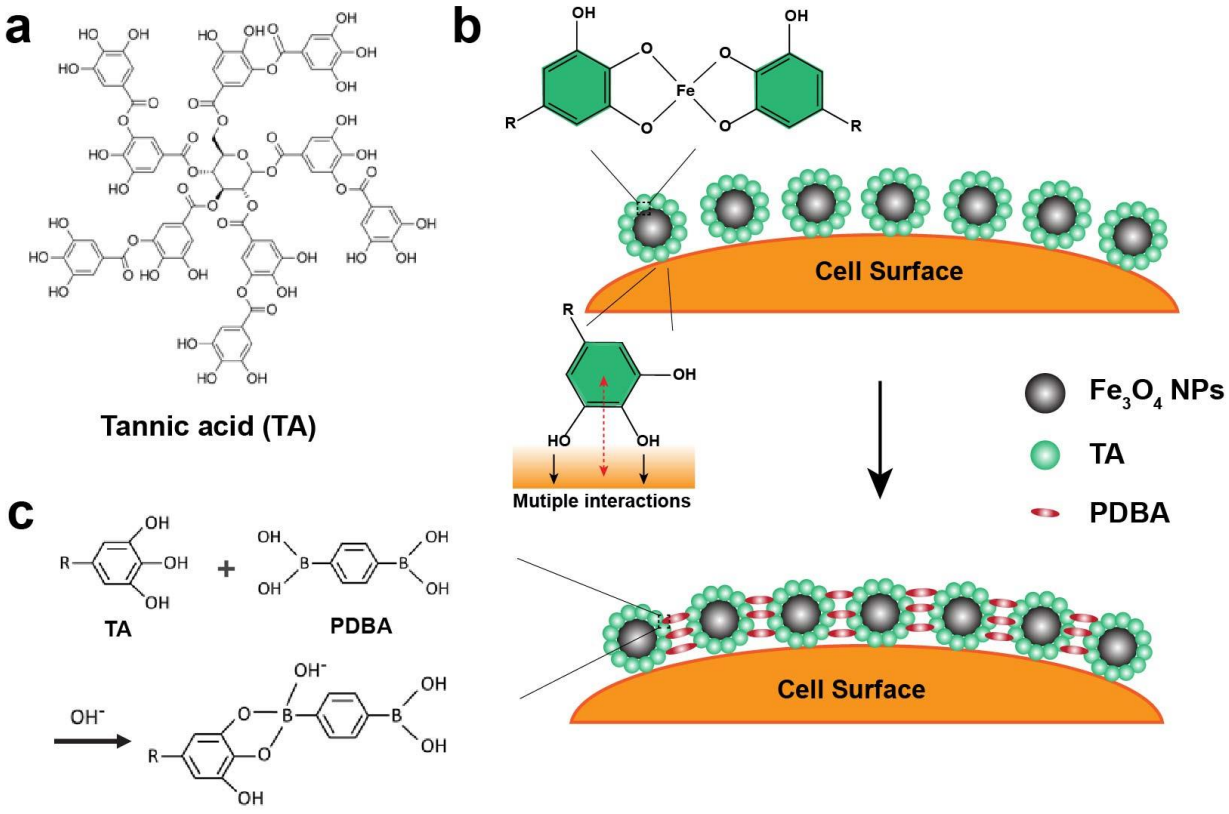

Figure S1. a) Molecular structure of TA. b) Metal (Fe)-phenolic interaction induced by TA. c) Reaction between TA and PDBA.

The proposed Janus cell modification of Fe_3O_4 was performed by first incubating cells with TA-treated Fe_3O_4 NPs, followed with adding PDBA. TA is a natural polyphenolic compound, composed of a central sugar molecule substituted with five digallic acid moieties (**Figure S1**a). TA can bind with plasma membranes via hydrophobic interactions and hydrogen bonds.[1] Their phenolic components are also widely utilized as the polydentate ligand to connect various metal ions through metal-phenolic coordination and induce metal–phenolic networks on the substrate (**Figure S1**b).[2] On the other hand, PDBA can rapidly react with TA and generate boronate ester thin films on the TA-modified template.[3] Therefore, in this study, TA acted as the bridge to connect cell membrane and Fe_3O_4 NPs, inducing a crosslinked metal-phenolic network of Fe_3O_4 NPs on the cell surface (**Figure S1b**). The adding of PDBA further form complexation between

phenylboronic acid (benzene-1,4-diboronic acid) and a phenolic building block (tannic acid) to rapidly assemble boronate ester, which crosslinks Fe_3O_4 NPs to form thin films on the surface of 293T cell (**Figure S1c**).Thus, TA built a bridge between cell membrane and Fe_3O_4 NPs, inducing a metal-phenolic network of Fe_3O_4 NPs on the cell surface. The resulting network was further crosslinked by adding PDBA, because the quick reaction between PDBA and TA can form boronate ester to crosslink TA, reinforcing the binding strength of the Fe_3O_4 complex. Regarding the fluidity of cell membranes, their motility is expected to significantly decrease when connected with the bulky Fe_3O_4 shell. Moreover, the diffusion of cell membrane is not supposed to dissociate the metal-coordinated Fe_3O_4 film with solid junctions. The modified magnetic layer may only diffuse as a crosslinked whole when cell membrane flow slowly. Therefore, the complexations between TA and cell membrane (hydrogen and hydrophobic interactions), TA and Fe_3O_4 NPs (metal-phenolic binding and crosslinking), TA and PDBA (boronate-phenolic covalent bond) generate an integrated network of Fe_3O_4 NPs with tight conjugation on the cell surface, facilitating the Janus cell robot to maintain its asymmetric structure despite the existing fluidity of cell membrane.

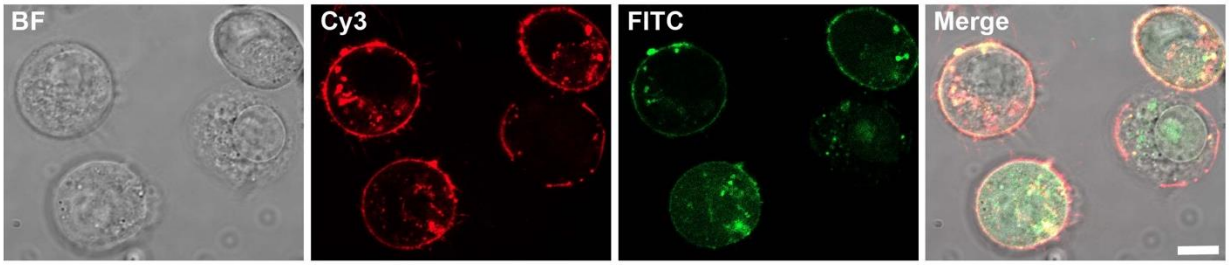

Figure S2. Bright-field (BF) and fluorescent images of 293T-R@OA cells modified with Cy3-labelled streptavidin and FITC-labelled cRGD. Scale Bar: 5 μm.

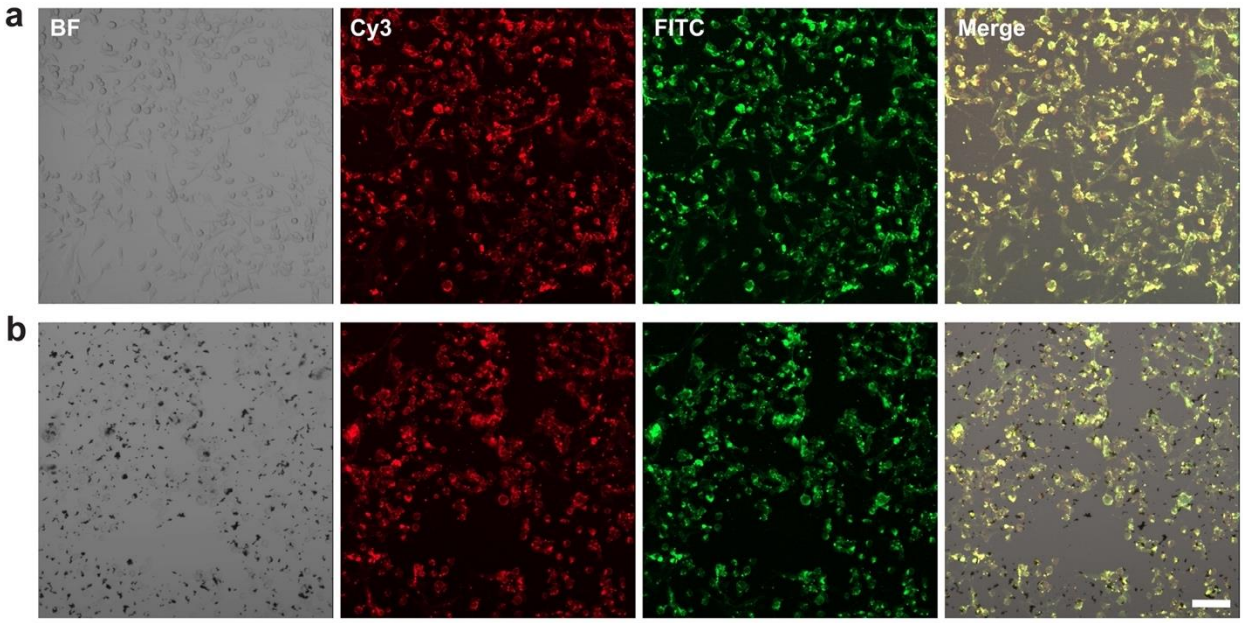

Figure S3. Bright-field (BF) and fluorescent images of 293T-R@OA cells that attached to the PLL-coated substrate (a) before and (b) after the Janus modification of Fe_3O_4 NPs. Scale Bar: 50 μm.

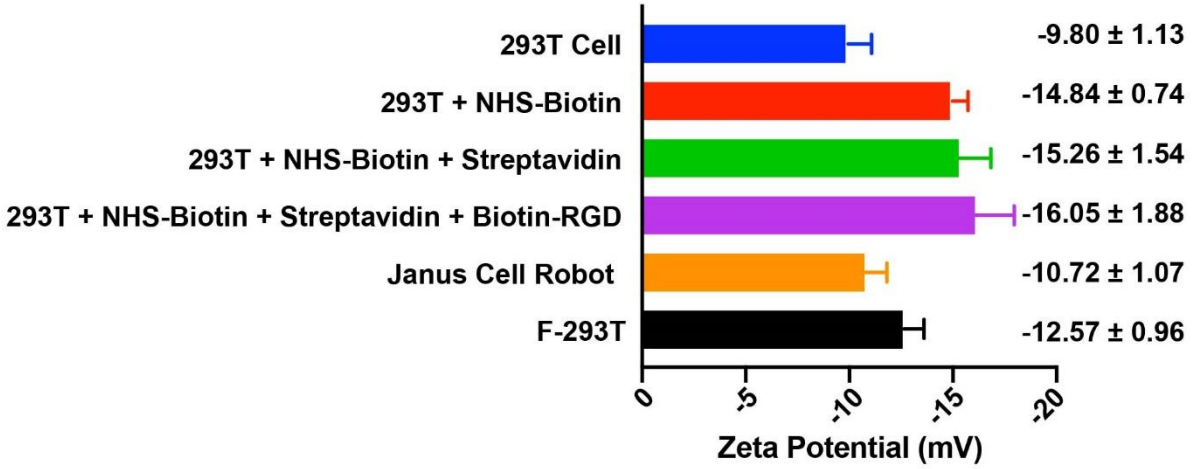

Figure S4. Zeta potential of the cell surface upon sequential surface modifications (n = 3, mean ± SD). F-293T: cells fully coated with cRGD and Fe_3O_4 NPs.

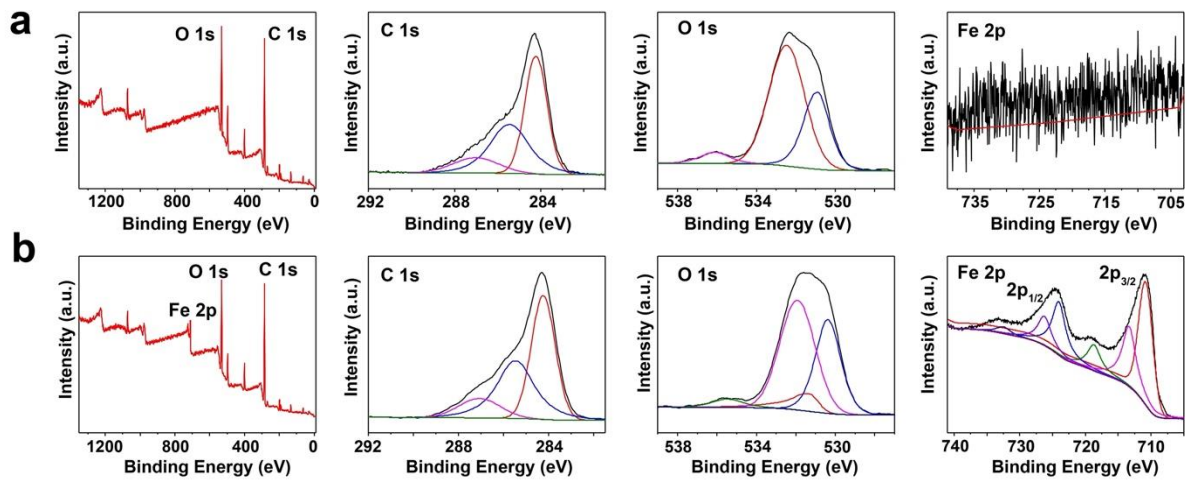

Figure S5. XPS spectra of wide scan, high-resolution C 1s, O 1s and Fe 2p: (a) 293T cells; (b) Janus cell robots.

As illustrated in **Figure S**5, the peak of Fe 2p was not observed in bare 293T cells. Whereas the Fe 2p spectrum of Janus cell robots showed two main peaks at 711.0 eV for Fe $2p_{3/2}$ and 724.6 eV for Fe $2p_{1/2}$, representing the typical peaks of Fe_3O_4. The Fe 2p peaks can be divided into three Fe^{2+} peaks ($2p_{3/2}$: 710.8 eV; satellite: 718.7 eV and $2p_{1/2}$: 724.0 eV) and three Fe^{3+} peaks ($2p_{3/2}$: 713.3 eV; $2p_{1/2}$: 726.2 eV and satellite: 732.5 eV).[4]

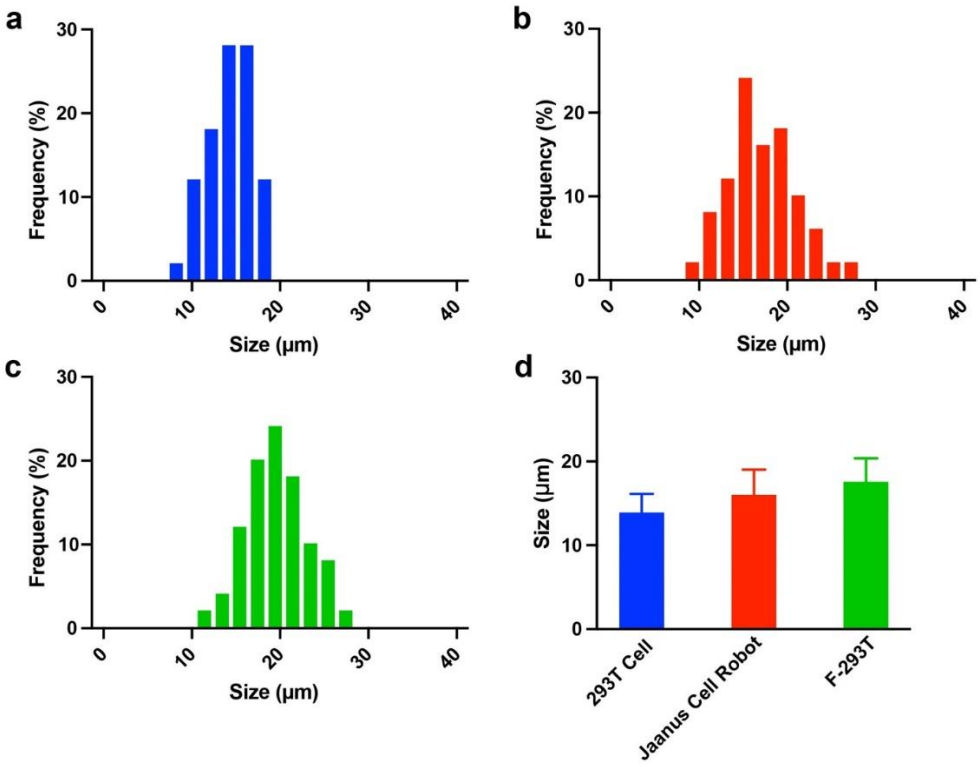

Figure S6. Size distribution of (a) unmodified 293T cells, (b) Janus cell robots and (c) F-293T cells, and (d) their calculated average size (n = 50, mean ± SD).

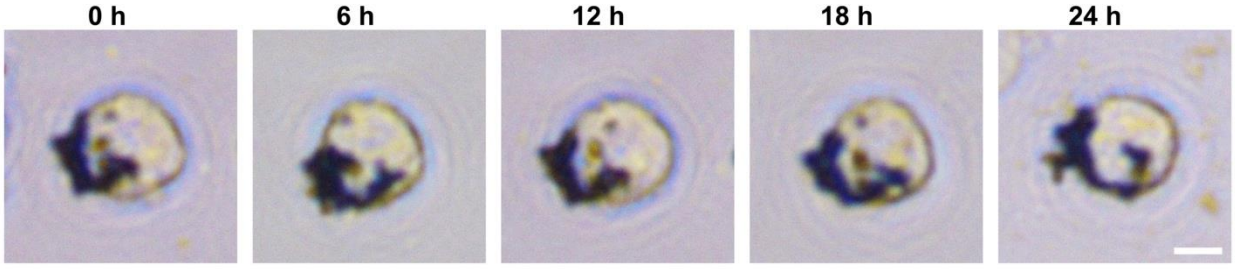

Figure S7. Time-lapse optical images of Janus cell robots over 24 hours. Scale bar: 5 μm.

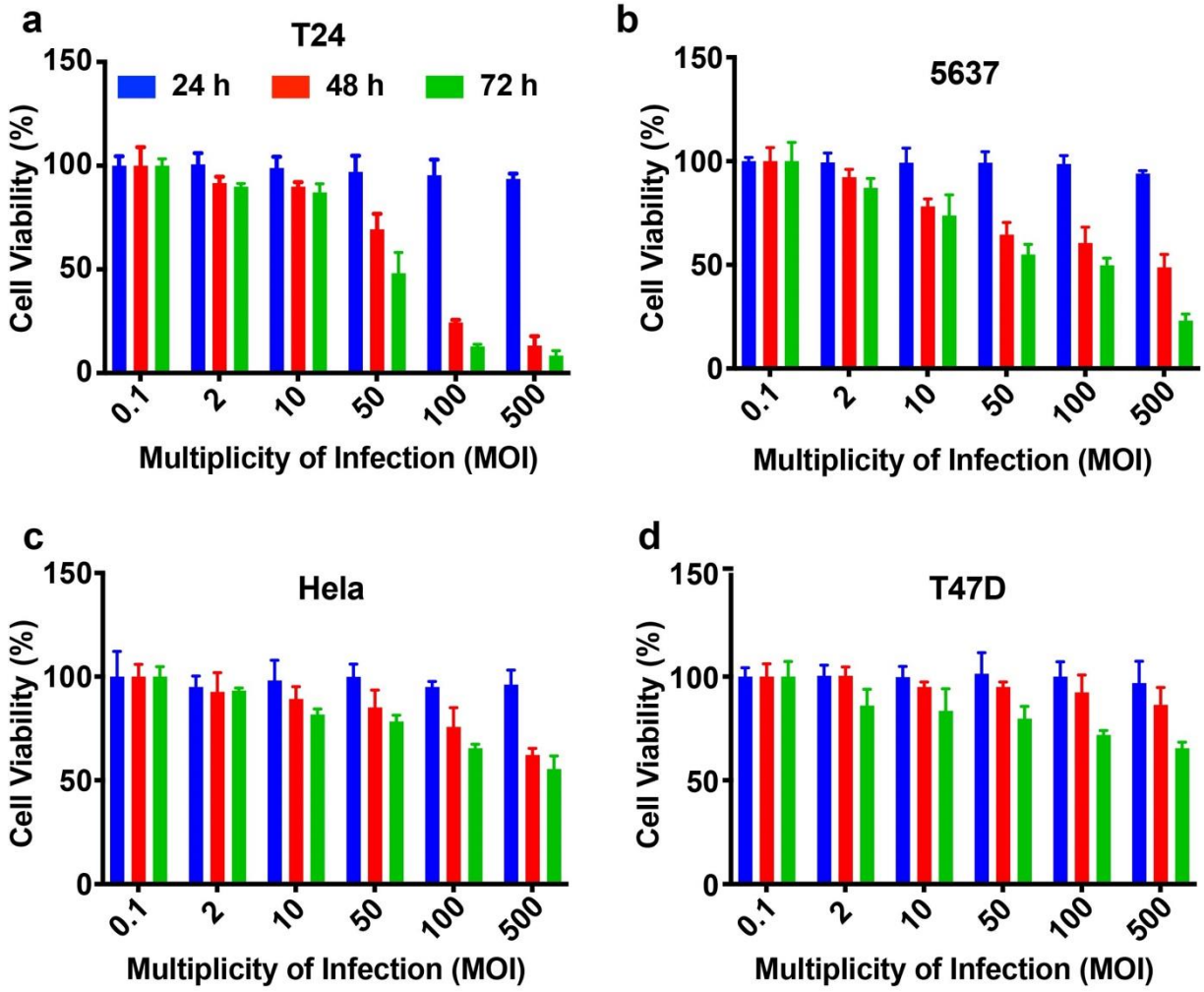

Figure S8. Viability of various cancer cells infected with different MOIs of OA after incubated for 24, 48 and 72 hours: a) T24 bladder cancer cells; b) 5637 bladder cancer cells; c) Hela cervical cancer cells; d) T47D breast cancer cells (n = 3; mean ± SD).

Various cancer cells were selected to infect with OA at different multiplicities of infection (MOIs) to examine the oncolytic effect of free OA. The viability of T24 bladder cancer cells after different incubation time is shown in Figure S8a. Only slight decrease on cell viability was observed at lower OA dose from 0.1 to 10 MOI after incubated for 72 hours. When the OA dose increased from 50 to 500 MOI, the cell viability exhibited significant decline after 48-hour postinfection, reflecting that T24 cells were susceptible to OA at higher dosages and lysed by the cytopathic effects of the infected and replicated OA. The cell viability of other three types of cells, 5637 bladder cancer cells, HeLa cervical cancer cells and T47D breast cancer cells, were

also evaluated after infected with OA at various MOIs. Similar trend was obtained in Figure S7b for 5637 cells, where OA at the dosage from 50 to 500 MOI presented high oncolysis effect after incubated for 48 hours. Whereas HeLa and T47D cells in Figure S8c-d, respectively, did not show efficient susceptibility to OA infection and over 50 % cells were still alive even infected with OA at 500 MOI after 72 hours postinfection. Such results reveal that bladder cancer cells are more sensitive to the infection and cytolysis of the selected OA compared to other cancer cell lines, encouraging us to apply Janus cell robots in bladder cancer treatment.

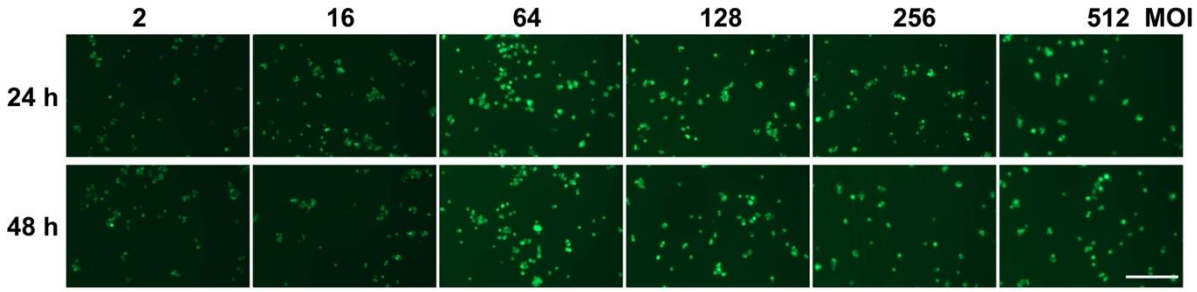

Figure S9. Fluorescent images of 293T cells infected with GFP-OA upon various MOIs after 24 and 48-hour postinfection. Scale bar: 50 μm.

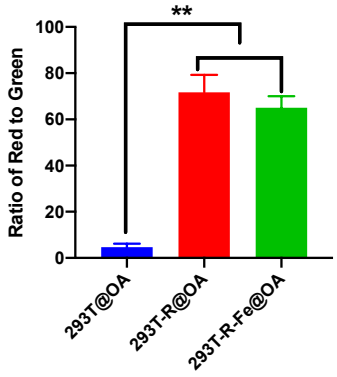

Figure S10. Ratio of quantified fluorescent intensity of DiD (red)-labeled 293T@OA, 293T-R@OA or 293T-R-Fe@OA cell robots to GFP-expressing (green) T24 cells after co-incubation for 1 hour (n = 3, mean ± SD). ***P* < 0.01, ANOVA.

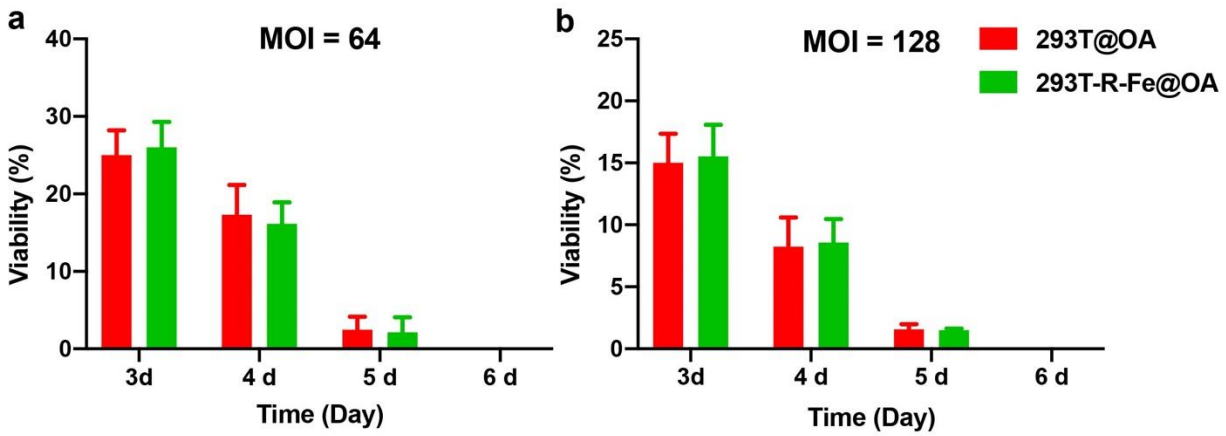

Figure S11. Viability of 293T@OA and 293T-Fe-R@OA cell robots with elongated incubation from 3 to 6 days upon different MOIs of OA: (a) 64 MOI; (b) 128 MOI (n = 3; mean ± SD).

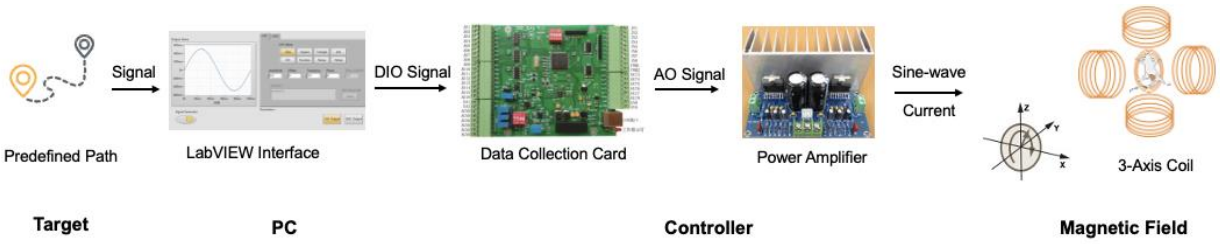

Figure S12. Schematic of the custom designed magnetic actuation system: a host computer with LabVIEW software, data collection card, power amplifier with AC power supply and 5 electromagnetic coils (a pair of coils in X and Y axis and one coil in Z axis).

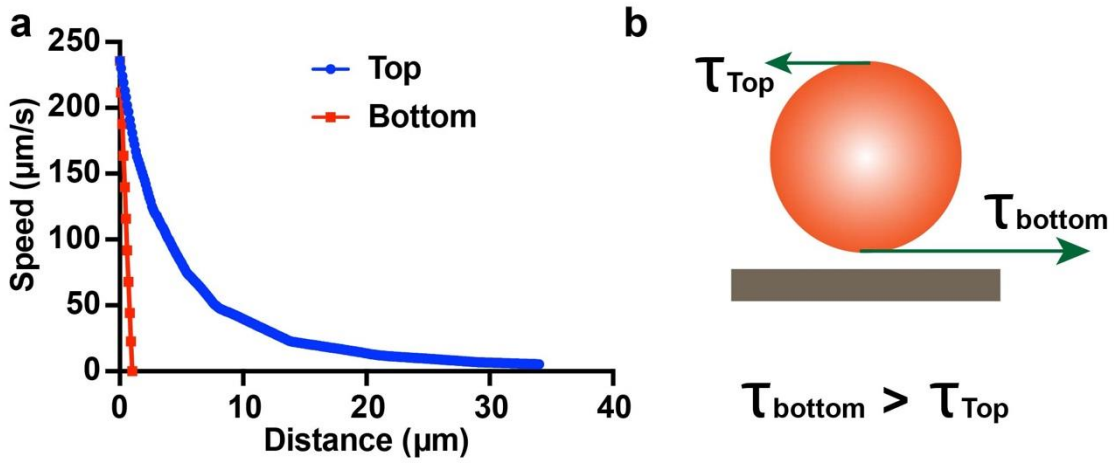

Figure S13. (a) Fluid flow speed around the top and bottom of the rotating Janus cell robot. (b) The mismatched hydrodynamic shear force on the top (τ_{top}) and bottom (τ_{bottom}) of the cell robot.

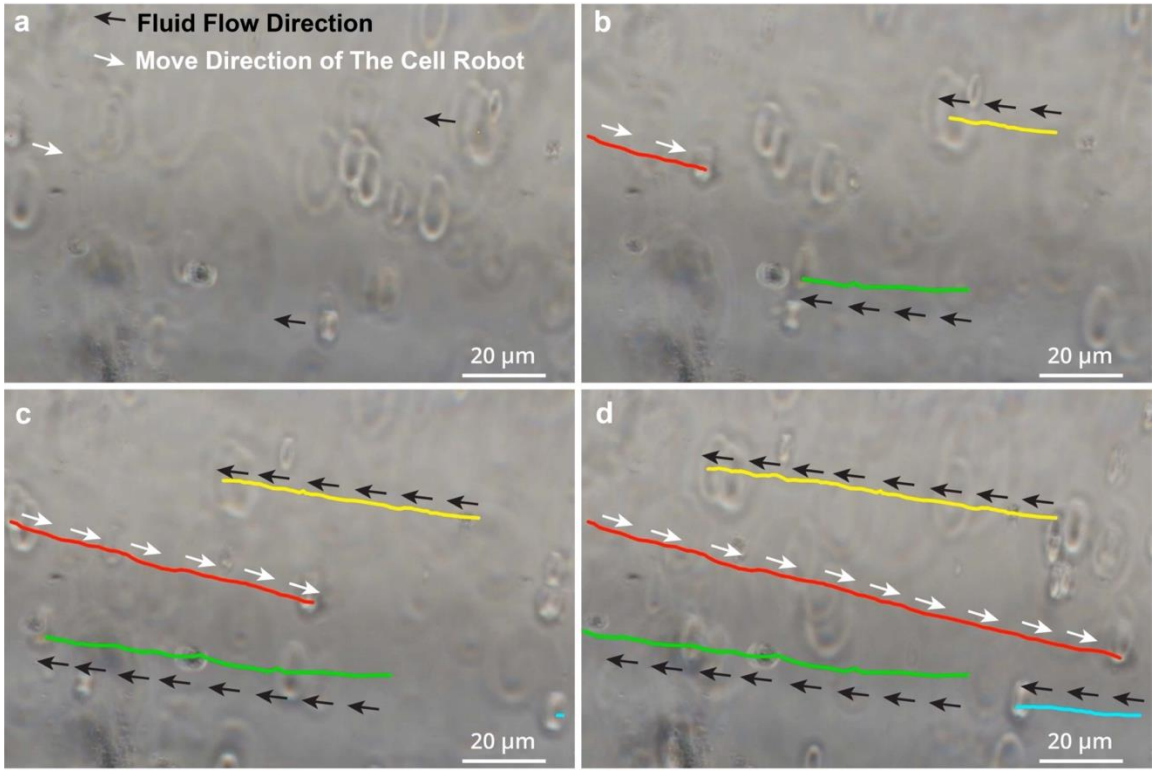

Figure S14. Time-lapse image exhibiting the magnetic propulsion of the cell robot against fluid flow. a) t = 0 s; b) t = 3 s; c) t = 6 s; d) t = 9 s. Scale bar: 20 μm.

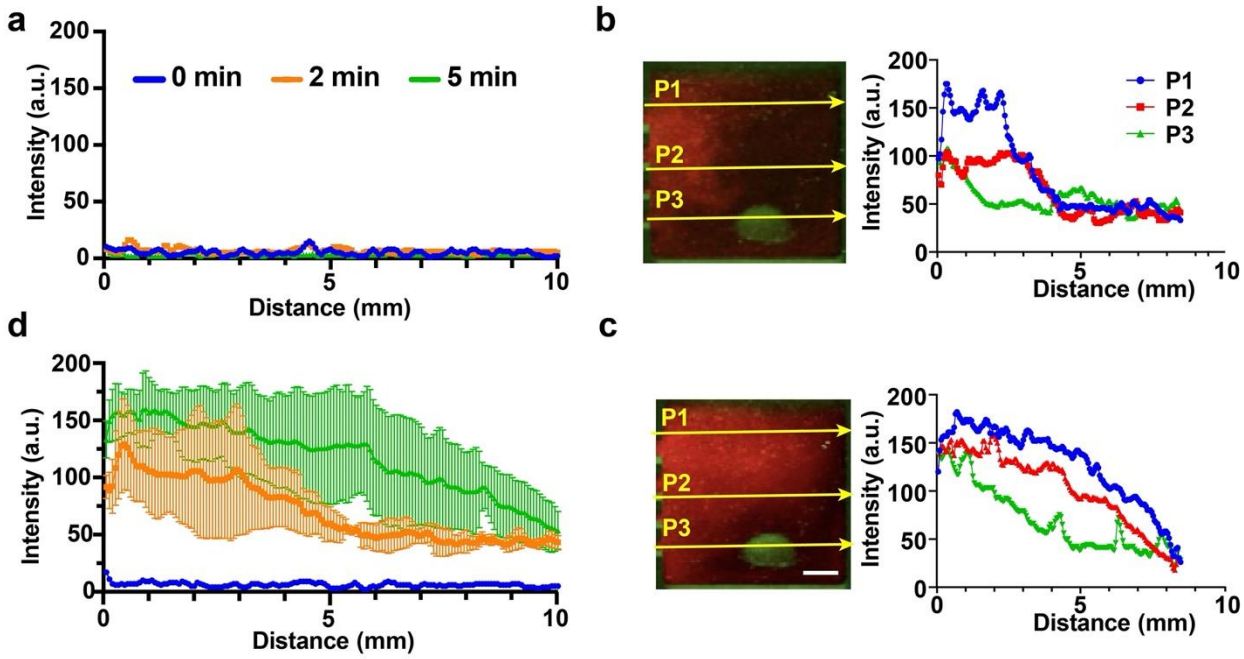

Figure S15. The average fluorescent intensity of Cy3-labelled cell robots that distributed along selected lines in the right chamber without (a) or with (d) RMF manipulation. Lines selected in the right chamber and corresponding fluorescent intensity distributed along selected lines of Cy3-labelled cell robots migrated from left side of the microfluidic device under RMF control for (b) 2 min and (c) 5 min. Scale bar: 2 mm.

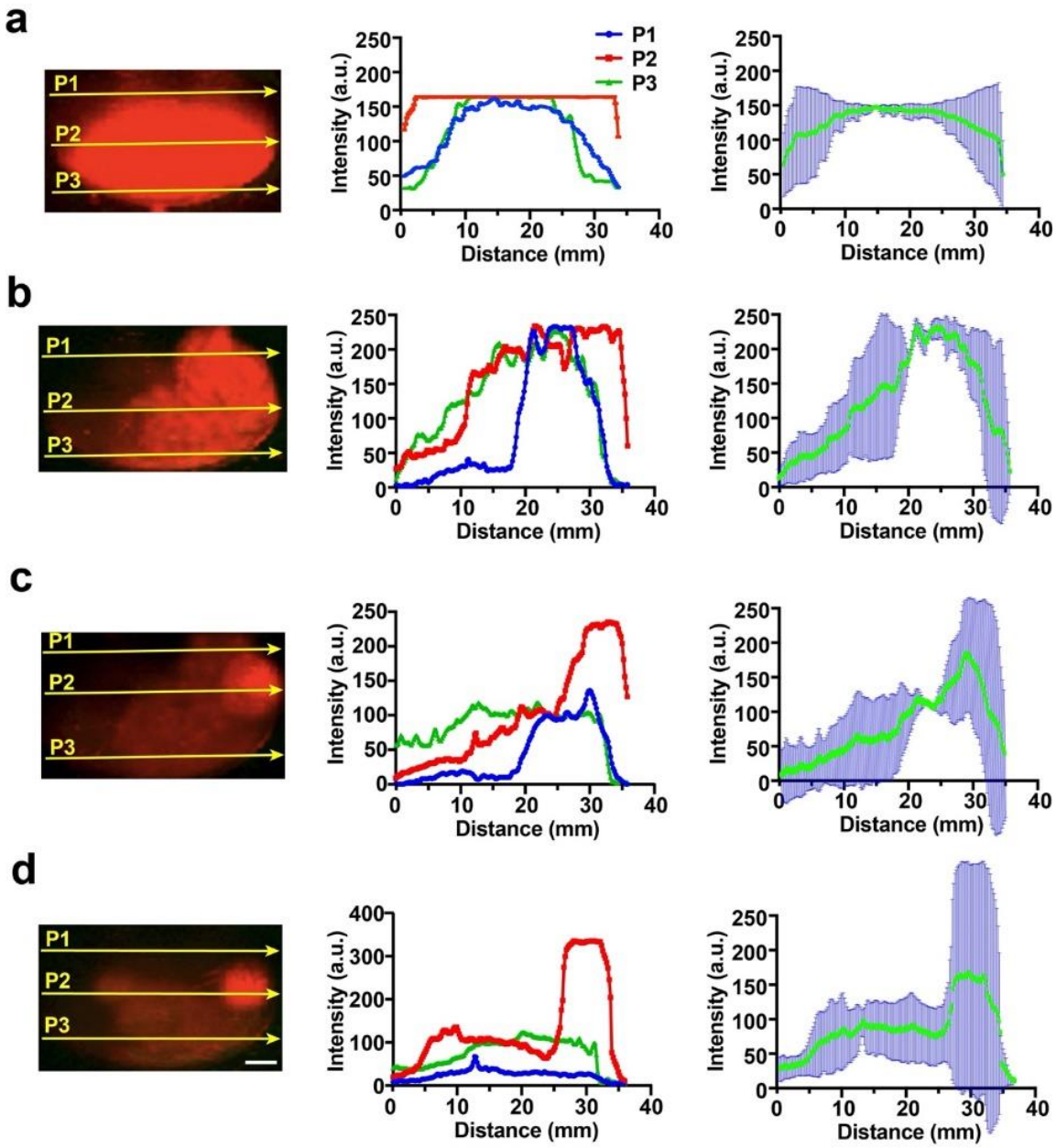

Figure S16. Lines selected in the bladder mold and corresponding each and average fluorescent intensity of Cy3-labelled cell robots distributed along selected lines under RMF control for (a) 0 min, (b) 2 min, (c) 5 min, and (d) 10 min. Scale bar: 10 mm.

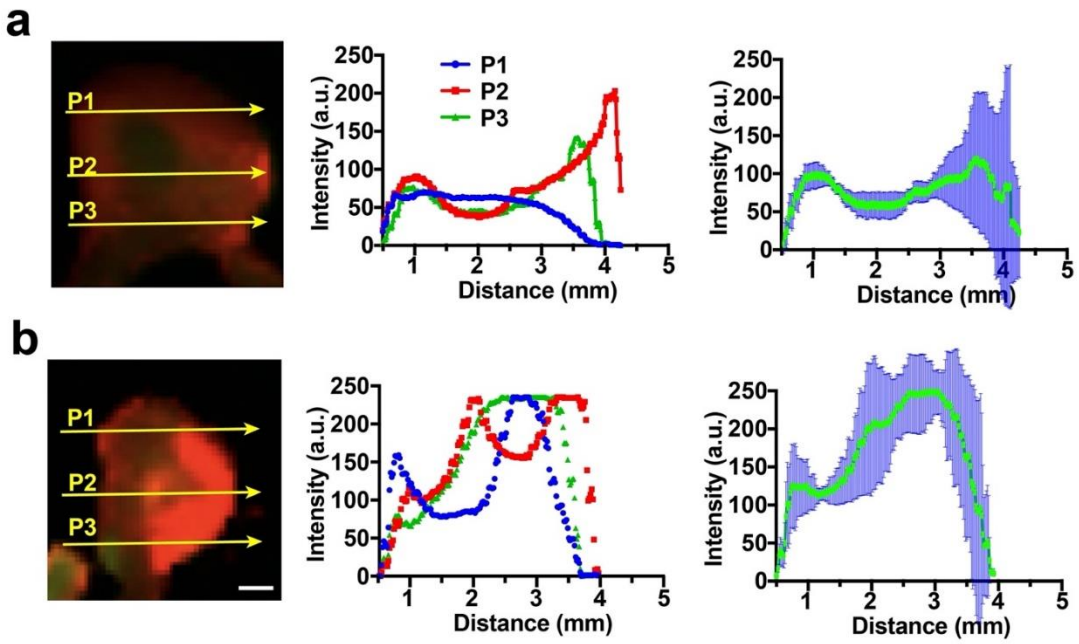

Figure S17. Lines selected in the dissected bladder and corresponding each and average fluorescent intensity of Cy5-labelled cell robots distributed along selected lines (a) without or (b) with RMF control for 60 min. Scale bar: 1 mm.

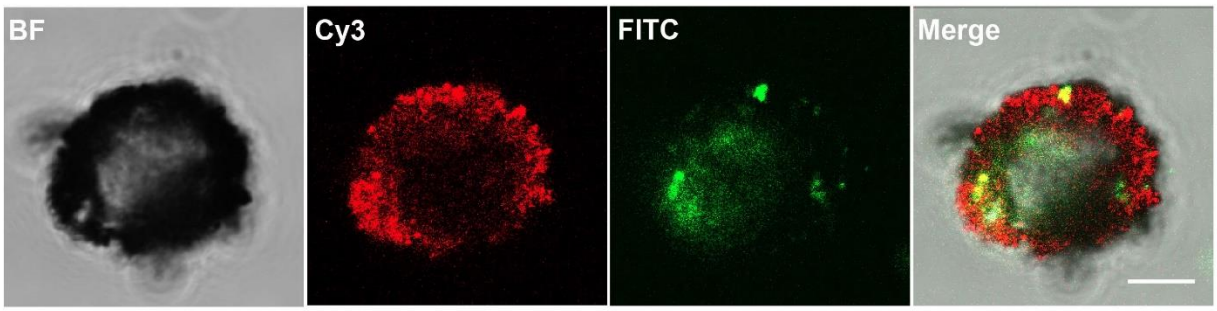

Figure S18. Bright-field (BF) and fluorescent images of F-293T cells with Cy3-labeled streptavidin and FITC-labeled cRGD. Scale Bar: 5 μm.

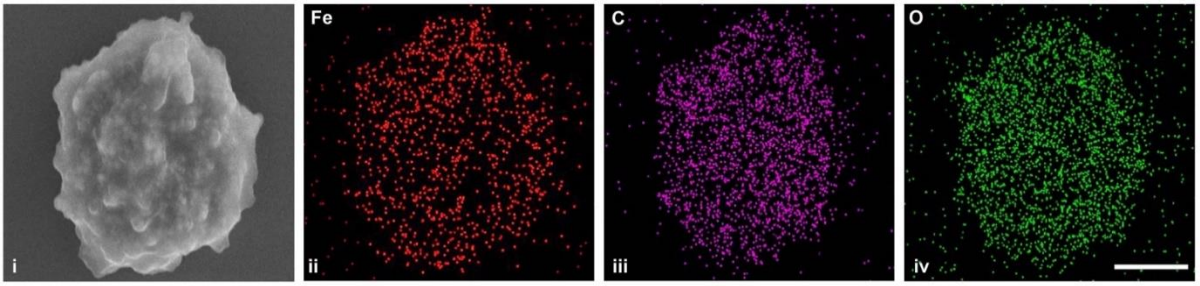

Figure S19. SEM (i) and EDX (ii-iv) images of F-293T cells. Scale bar: 5 μm.

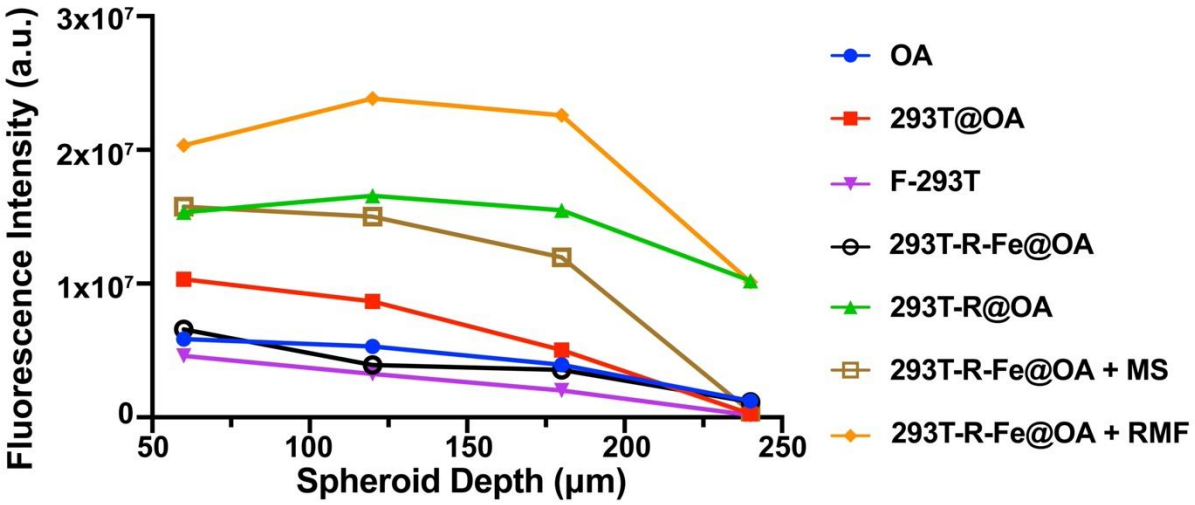

Figure S20. Fluorescence intensity of GFP in transverse sections at different spheroid depths upon various culture conditions.

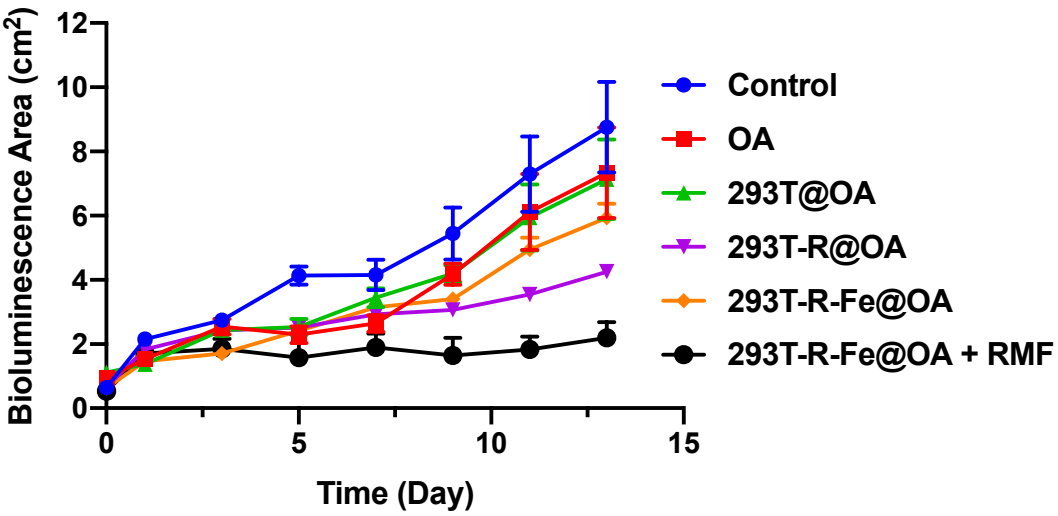

Figure S21. Bioluminescence area of T24 bladder tumor-bearing mice under various intravesical administrations over the treatment course (n = 5; mean ± SD).

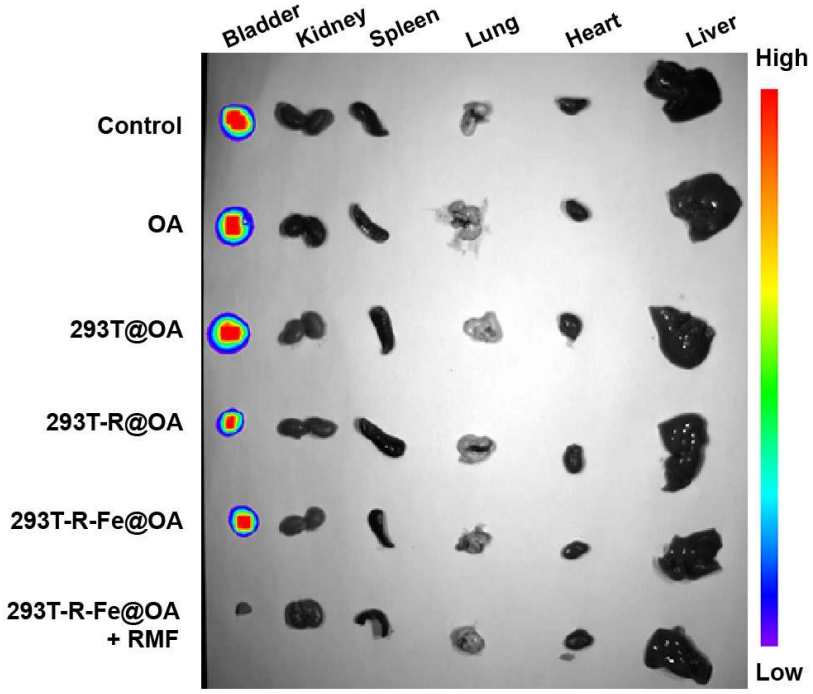

Figure S22. Representative bioluminescence images of bladder and other major organs dissected from T24 tumor-bearing mice under various intravesical administrations after the treatment course (day 13).

References

[1] a) S. Simon, E. Disalvo, K. Gawrisch, V. Borovyagin, E. Toone, S. Schiffman, D. Needham, T. McIntosh, *Biophys. J.* **1994**, *66*, 1943; b) H. Wang, C. Wang, Y. Zou, J. Hu, Y. Li, Y. Cheng, *Giant* **2020**, *3*, 100022.

[2] a) W. Zhu, G. Xiang, J. Shang, J. Guo, B. Motevalli, P. Durfee, J. O. Agola, E. N. Coker, C. J. Brinker, *Adv. Funct. Mater.* **2018**, *28*, 1705274; b) J. Guo, Y. Ping, H. Ejima, K. Alt, M. Meissner, J. J. Richardson, Y. Yan, K. Peter, D. Von Elverfeldt, C. E. Hagemeyer, *Angew. Chem. Int. Ed.* **2014**, *53*, 5546.

[3] J. Guo, H. Sun, K. Alt, B. L. Tardy, J. J. Richardson, T. Suma, H. Ejima, J. Cui, C. E. Hagemeyer, F. Caruso, *Adv. Healthc. Mater.* **2015**, *4*, 1796.

[4] a) Koo, H. Hong, P. W. Im, H. Kim, C. Lee, X. Jin, B. Yan, W. Lee, H.-J. Im, S. H. Paek, *Nano Converg.* **2020**, *7*, 1; b) X. Q. Tang, Y. D. Zhang, Z. W. Jiang, D. M. Wang, C. Z. Huang, Y. F. Li, *Talanta* **2018**, *179*, 43.